

Extremal Behavior of Aggregated Data with an Application to Downscaling

Sebastian Engelke*, Raphaël de Fondeville[†] and Marco Oesting[‡]

March 15, 2022

Abstract

The distribution of spatially aggregated data from a stochastic process X may exhibit a different tail behavior than its marginal distributions. For a large class of aggregating functionals ℓ we introduce the ℓ -extremal coefficient that quantifies this difference as a function of the extremal spatial dependence in X . We also obtain the joint extremal dependence for multiple aggregation functionals applied to the same process. Explicit formulas for the ℓ -extremal coefficients and multivariate dependence structures are derived in important special cases. The results provide a theoretical link between the extremal distribution of the aggregated data and the corresponding underlying process, which we exploit to develop a method for statistical downscaling. We apply our framework to downscale daily temperature maxima in the south of France from a gridded data set and use our model to generate high resolution maps of the warmest day during the 2003 heatwave.

Keywords: Aggregation; Geostatistics; Simulation of extreme events; Spatial extremes; Threshold exceedance.

1 Introduction

Spatial extreme value theory and, especially, max-stable processes are widely applied tools to assess risks in environmental science. These processes are motivated by the study of

$$M_n(s) = \max_{i=1,\dots,n} \frac{X_i(s) - b_s(n)}{a_s(n)}, \quad s \in S, \quad (1)$$

where X_1, \dots, X_n are independent observations of a sample-continuous process X , modeling a phenomenon of interest such as rainfall or temperature on some region S . The scaling functions $a_s(n) > 0$ and $b_s(n) \in \mathbb{R}$, $n \in \mathbb{N}$, are both continuous in $s \in S$. Functional limits obtained from this construction as $n \rightarrow \infty$, named the class of max-stable processes, are appealing models for spatial extremes. Their realizations, however, are composed of different single events X_i , which prohibits direct interpretation and renders efficient inference and simulation challenging [e.g., Dombry et al., 2016, Thibaud et al., 2016]. It is often more natural to study threshold exceedances, or, more precisely, the extremal behavior of $\ell(X_i)$, $i = 1, \dots, n$, where ℓ is a functional on the space of continuous functions on S . Buishand et al. [2008],

*École Polytechnique Fédérale de Lausanne, EPFL-FSB-MATHAA-STAT, Station 8, 1015 Lausanne, Switzerland. Email: sebastian.engelke@epfl.ch

[†]École Polytechnique Fédérale de Lausanne, EPFL-FSB-MATHAA-STAT, Station 8, 1015 Lausanne, Switzerland. Email: raphael.de-fondeville@epfl.ch

[‡]Universität Siegen, Department Mathematik, Walter-Flex-Str. 3, 57068 Siegen, Germany. Email: oesting@mathematik.uni-siegen.de

for instance, consider the daily rainfall over a certain region S , and therefore choose $\ell(X) = \int_S X(s)ds$. Using the same functional, Coles and Tawn [1996] relate the tail of the distribution of the integral to the tail of the distribution at a single location, and Ferreira et al. [2012] formalize this idea through the so-called reduction factor. For general homogeneous functionals ℓ , Dombry and Ribatet [2015] characterize the functional limits of threshold exceedances $u^{-1}X \mid \ell(X) > u$, for a high threshold u .

In this paper we follow the approach of Coles and Tawn [1996] and Ferreira et al. [2012] in order to investigate the tail behavior of more general functionals ℓ . Under certain conditions we show that, for any $s_0 \in S$,

$$\text{pr} \left[\frac{\ell(X) - \ell\{b_s(n)\}}{\ell\{a_s(n)\}} > x \right] \approx \theta^\ell \text{pr} \left\{ \frac{X(s_0) - b_{s_0}(n)}{a_{s_0}(n)} > x \right\}, \quad x \in \mathbb{R}, \quad (2)$$

for sufficiently large n . This means that the tail of the ℓ -functional of X behaves like the tail at an individual location times a reduction factor θ^ℓ , which we call the ℓ -extremal coefficient. In different contexts, the interpretation of this coefficient might differ, but intuitively θ^ℓ summarizes the effect of spatial extremal dependence in X on the risk diversification through the functional ℓ .

The ℓ -extremal coefficient relates the tail of the univariate random variable $\ell(X)$ to the multivariate or spatial extremal dependence in X . A major advantage of this functional perspective is that it produces return level estimates that are consistent with respect to the underlying structure of X , even when considering different aggregation functionals applied to the same process X . Indeed, for functionals ℓ_1, \dots, ℓ_L , we study the multivariate tail behavior of $(\ell_1(X), \dots, \ell_L(X))$, which turns out to be in the max-domain of attraction of a multivariate max-stable distribution.

Popular models for the functional limit of the maxima M_n in (1) are Brown–Resnick processes that take a similar role in spatial extremes as Gaussian processes in classical geostatistics. The reason for this is that the former are essentially the only such limits when X is a stationary Gaussian process and an additional rescaling is allowed [Kabluchko et al., 2009]. This connection can be exploited to perform efficient inference [Wadsworth and Tawn, 2014, Engelke et al., 2015, Thibaud et al., 2016] and simulation [Dombry et al., 2013, 2016, Oesting and Strokorb, 2017] for Brown–Resnick processes based on densities and sampling algorithms of Gaussian random vectors. In our framework, this link to Gaussian distributions allows us to use results from the geostatistical literature on data aggregation [e.g., Wackernagel, 2003] to obtain explicit expressions for θ^ℓ and the extremal dependence in $(\ell_1(X), \dots, \ell_L(X))$ if the limiting process Z in (1) is a Brown–Resnick process with Gumbel margins.

An important consequence of our findings is that they allow, under certain assumptions, to recover the tail distribution of X based only on information from the aggregated vector. This is similar to inferring the extremal dependence of X based only on extremal coefficients [cf., Schlather and Tawn, 2003]. In meteorology, for instance, large scale climate models provide only data over grid cells, but practical questions require risk assessment at point locations such as cities or other infrastructural sites. Techniques to perform this transition from large to small scales are summarized under the notion of downscaling. In the second part of the paper we thus propose a statistical downscaling method to infer in a spatially consistent way the tail behavior of the underlying stochastic process X based on the observed extremes of the aggregated data. Relevant outputs will be the exceedance probabilities at point locations and simulations of spatial extreme events of X , both unconditionally and conditionally on the observed aggregated extremes. We apply this procedure to coarse scale gridded temperature data in the south of France from the e-obs data set [Haylock et al., 2008]. The fitted model provides, for instance, fine-resolution simulations of the warmest day during the 2003 heatwave conditionally on the observed grid values.

2 Limit results for extremes of aggregated data

2.1 Background on extremes

Let S be a compact subset of a complete separable metric space. By $C(S)$ we denote the space of real-valued functions on S equipped with the supremum norm $\|\cdot\|_\infty$, defined by $\|f\|_\infty = \sup_{s \in S} |f(s)|$, and the corresponding Borel σ -algebra $\mathcal{C}(S)$.

We consider a sample-continuous stochastic process $\{X(s), s \in S\}$, which we assume to be in the max-domain of attraction of a max-stable process with common marginal extreme value index $\xi \in \mathbb{R}$. More precisely, for independent copies X_1, \dots, X_n of X , there exist functions $a_s : (0, \infty) \rightarrow (0, \infty)$, $b_s : (0, \infty) \rightarrow \mathbb{R}$, both continuous in $s \in S$, such that as $n \rightarrow \infty$, the process M_n of componentwise maxima defined in (1) converges in distribution on the space $C(S)$, i.e.,

$$\mathcal{L} \left\{ \max_{i=1, \dots, n} \frac{X_i(s) - b_s(n)}{a_s(n)}, s \in S \right\} \longrightarrow \begin{cases} \mathcal{L}\{\text{sgn}(\xi)Z(s)^\xi, s \in S\}, & \xi \neq 0, \\ \mathcal{L}\{\log Z(s), s \in S\}, & \xi = 0, \end{cases} \quad (3)$$

where $\mathcal{L}(\eta)$ denotes the law of a process η . By definition, the process Z in the limit is max-stable, and it is simple in the sense that it is normalized to have unit Fréchet margins [cf., de Haan and Ferreira, 2006, Chapter 9]. Moreover, for any $s \in S$, the margin $X(s)$ then is in the max-domain of attraction of an extreme value distribution

$$G_\xi(x) = \begin{cases} \exp[-\{\text{sgn}(\xi)x\}^{-1/\xi}], & \xi \neq 0, \\ \exp\{-\exp(-x)\}, & \xi = 0, \end{cases} \quad (4)$$

for all $x\xi \geq 0$. The different distributions are called $(1/\xi)$ -Fréchet for $\xi > 0$, Gumbel for $\xi = 0$ and $(-1/\xi)$ -Weibull for $\xi < 0$, respectively. The assumption of a spatially constant ξ in (3) is common in the literature since it is required to obtain meaningful theoretical results, and it is usually a reasonable hypothesis in applications.

According to its spectral representation [cf. de Haan, 1984, Giné et al., 1990, Penrose, 1992],

$$Z(s) = \max_{i \in \mathbb{N}} U_i W_i(s), \quad s \in S, \quad (5)$$

where $\{U_i, i \in \mathbb{N}\}$ are the points of a Poisson point process on $(0, \infty)$ with intensity measure $u^{-2} du$ and the spectral functions $W_i, i \in \mathbb{N}$, are independent copies of some non negative sample-continuous process $\{W(s), s \in S\}$ with $E\{W(s)\} = 1$ for all $s \in S$.

In the sequel we assume that X is non negative for the Fréchet case $\xi > 0$, while for the Weibull case $\xi < 0$ each $X(s), s \in S$, is assumed to have the same upper endpoint 0. Finally, we provide the example of the widely used class of Brown–Resnick max-stable processes.

EXAMPLE 1. Let $\{G(s) : s \in S\}$ be a centered Gaussian process with variogram $\gamma(s, t) = \text{var}\{G(s) - G(t)\}$. A Brown–Resnick process is the max-stable process Z in (5) where the spectral functions follow the distribution of

$$W(s) = \exp[G(s) - \text{var}\{G(s)\}/2], \quad s \in S.$$

The distribution of Z only depends on the variogram γ , and for $s_1, \dots, s_m \in S$, the finite dimensional distribution of $(Z(s_1), \dots, Z(s_m))$ is called the Hüsler–Reiss distribution [Hüsler and Reiss, 1989] with parameter matrix $\Gamma = \{\gamma(s_j, s_k)\}_{j,k=1, \dots, m}$; more details can be found in Appendix B and in Brown and Resnick [1977], Kabluchko et al. [2009] and Kabluchko [2011].

2.2 Univariate limiting distributions of aggregated data

We first derive the univariate asymptotic distribution of aggregated data. Following Ferreira et al. [2012], we assume that the normalizing functions $a_s(t)$ can be decomposed asymptotically into positive functions $A(s)$ and $a(t)$ in the sense that

$$\sup_{s \in S} \left| \frac{a_s(t)}{a(t)} - A(s) \right| \rightarrow 0, \quad \text{as } t \rightarrow \infty. \quad (6)$$

In the Gumbel case $\xi = 0$, the left-hand side of (6) is even assumed to be equal to zero, i.e.,

$$a_s(t) = A(s)a(t) \quad \text{for all } s \in S, t > 0. \quad (7)$$

For data aggregation, we consider a positively homogeneous functional $\ell : C(S) \rightarrow \mathbb{R}$, i.e., ℓ satisfies $\ell(af) = a\ell(f)$ for all $a > 0, f \in C(S)$. We further assume that ℓ is uniformly continuous, and we use the notation $\ell(f)$ and $\ell\{f(s)\}$ interchangeably.

The following theorem is a particular case of Theorem 2, that is proved in Section 2.3. Alternatively it can be proved similarly to Ferreira et al. [2012, Theorem 2.1].

Theorem 1. *Let ℓ be a positively homogeneous and uniformly continuous functional on $C(S)$. Further, assume that (3) and (6) hold. If $\xi \leq 0$, the spectral functions W belonging to the process Z in (3) are assumed to be strictly positive. Then, for $\xi \neq 0$, we have*

$$\lim_{t \rightarrow \infty} t \, \text{pr} \left[\frac{\ell(X)}{a(t)\ell\{A(s)\}} > x \right] = \theta_\xi^\ell |x|^{-1/\xi}, \quad \xi > 0, \quad (8)$$

where

$$\theta_\xi^\ell = E \left(\left[\frac{\ell\{W(s)^\xi A(s)\}}{\ell\{A(s)\}} \right]^{1/\xi} \right). \quad (9)$$

For $\xi = 0$, we further require that (7) holds and that ℓ is linear. In this case,

$$\lim_{t \rightarrow \infty} t \, \text{pr} \left[\frac{\ell(X) - \ell\{b_s(t)\}}{a(t)\ell\{A(s)\}} > x \right] = \theta_0^\ell \exp(-x), \quad x \in \mathbb{R}, \quad (10)$$

where

$$\theta_0^\ell = E \left\{ \exp \left(\frac{\ell\{\log[W(s)]A(s)\}}{\ell\{A(s)\}} \right) \right\}. \quad (11)$$

REMARK 1. *Theorem 1 is formulated for threshold exceedances, but, using well-known equivalences from univariate extreme value theory, it could be easily reformulated to describe the limiting behavior of $\max_{i=1}^n \ell(X_i)$, where X_1, \dots, X_n are independent copies of X .*

We call the quantity θ_ξ^ℓ the ℓ -extremal coefficient since it describes the change of the upper tail of the ℓ -aggregated data compared to the tail of the univariate marginal data. Our definition of θ_ξ^ℓ in Theorem 1 contains a normalization by $\ell\{A(s)\}$, making it invariant under multiplication of ℓ by a constant and thus simplifying interpretation. Indeed, for $\xi > 0$ and $s_0 \in S$, we observe that

$$\theta_\xi^\ell = \lim_{u \rightarrow \infty} \frac{\text{pr} \{ \ell(X)/\ell(A) > u \}}{\text{pr} \{ X(s_0)/A(s_0) > u \}}.$$

The interpretation of this coefficient might differ depending on the respective context and risk functional ℓ . In general, θ_ξ^ℓ summarizes the effect of the spatial extremal dependence in X on the diversification of

the risk through functional ℓ . Importantly, not only the dependence but also the marginal tail index ξ may effect the coefficient θ_ξ^ℓ , which we stress in Theorem 1 and henceforth by the index ξ .

The concept of the ℓ -extremal coefficient extends and unifies various notions in extreme value statistics and applied sciences such as extremal coefficients, diversification factors in portfolios and areal reduction factors. We present these and other examples for illustration, always assuming that X satisfies the conditions of Theorem 1.

EXAMPLE 2. *The important case where $S \subset \mathbb{R}^2$ is a compact region and $\ell(f) = 1/|S| \int_S f(s) ds$ was first studied in Coles and Tawn [1996] and Buishand et al. [2008] in the framework of total areal rainfall, and then formalized by Ferreira et al. [2012]. In this case of a spatial average, the coefficient $\theta_\xi^\ell = \theta_\xi^{\text{avg}}$ is popular in environmental science where it is called the areal reduction factor. Hydrologists use it to convert quantiles of point rainfall to quantiles of total rainfall over a river catchment of interest. Interestingly, this coefficient satisfies $0 < \theta_\xi^{\text{avg}} \leq 1$ for $\xi \leq 1$, and $\theta_\xi^{\text{avg}} \geq 1$ for $\xi \geq 1$ [Ferreira et al., 2012, Prop. 2.2]. That means that average rainfall is less extreme than point rainfall if the marginals have finite expectation, as typically encountered in practice, and more extreme if they have infinite expectation.*

EXAMPLE 3. *If $S = \{s_1, \dots, s_m\}$ is a finite set and $\ell(f) = \sum_{i=1}^m c_i f(s_i)$ is a weighted sum with fixed $c_1, \dots, c_m \geq 0$, then Zhou [2010] and Mainik and Embrechts [2013] computed the corresponding coefficient θ_ξ^ℓ for $\xi > 0$. In this setup, $X(s_i)$, $i = 1, \dots, m$, are interpreted as dependent, heavy-tailed risk factors, and θ_ξ^ℓ represents the diversification in the portfolio $P = \sum_{i=1}^m c_i X(s_i)$. More precisely, the value at risk of P for high levels $\alpha \rightarrow 1$ can be expressed as the value at risk of a single factor times a constant that involves the ℓ -extremal coefficient θ_ξ^ℓ . Theorem 1 yields an analogous result also for light tailed risk factors.*

EXAMPLE 4. *Another well-known example is the case of $S = \{s_1, \dots, s_m\}$ being a finite set and $\ell(f) = \max_{i=1}^m f(s_i)$. If we further have $A(s_1) = \dots = A(s_m)$, then $\theta_\xi^\ell = E \{\max_{i=1}^m W(s_i)\}$ corresponds to the classical extremal coefficient [Schlather and Tawn, 2003], a number between 1 and m that is usually interpreted as the number of asymptotically independent random variables among $X(s_1), \dots, X(s_m)$. A similar interpretation is valid also if S is an arbitrary compact subset, and $\theta_\xi^\ell = E \{\max_{s \in S} W(s)\}$ is a spatial extension of the classical extremal coefficient.*

EXAMPLE 5. *As a last example, we consider energy functionals of the type $\ell^2(f) = \int_S f(s)^2 ds$ that appear in various applications in physics. In the case of X being a wind field, $\ell^2(X)$ is proportional to the integrated kinetic energy over a region S , which is an indicator for the potential damage caused by the corresponding storm event [eg. Powell and Reinhold, 2007].*

The expressions (9) and (11) for the ℓ -extremal coefficient are expected values of functions of the spectral process W . The distribution of the latter is known for most popular models, and it includes truncated Gaussian processes [Schlather, 2002, Opitz, 2013] and log-Gaussian processes [Brown and Resnick, 1977, Kabluchko et al., 2009], for instance. Numerical evaluation of θ_ξ^ℓ is thus readily implemented through simulations of W . In the important case of $\xi = 0$ and W corresponding to a log-Gaussian process, we obtain a closed form expression for θ_0^{avg} .

EXAMPLE 6. *Suppose that $\xi = 0$ and Z is a Brown–Resnick process on a compact set $S \subset \mathbb{R}^d$, as introduced in Example 1. The extremal coefficient of the spatial average then is*

$$\log \theta_0^{\text{avg}} = - \frac{\int_S \int_S A(s) A(t) \gamma(s, t) ds dt}{4 \left\{ \int_S A(s) ds \right\}^2}. \quad (12)$$

Let $d = 1$ and $S = [0, T]$, $T > 0$, and consider the popular power variogram model, namely $\gamma(s, t) = |(s - t)/\lambda|^\alpha$ for some $\alpha \in (0, 2]$, $\lambda > 0$. In this case we obtain

$$\theta_0^{avg} = \exp \left\{ -\frac{T^\alpha}{2\lambda^\alpha(\alpha + 1)(\alpha + 2)} \right\}.$$

2.3 Multivariate limiting distributions of aggregated data

In the previous section we derived the univariate tail distribution of data aggregated through a functional ℓ . In applications we often observe data through several different functionals, e.g., the integrals over not necessarily disjoint areas. The consistency of return level estimates discussed in the introduction has even more important implications when different risk functionals are applied to the data. The univariate tail of each aggregation could be estimated separately, but the dependence between the tails would not be captured. We consider therefore arbitrary positively homogeneous, uniformly continuous functionals $\ell_1, \dots, \ell_L : C(S) \rightarrow \mathbb{R}$, and we aim at describing the multivariate tail behavior of the vector $(\ell_1(X), \dots, \ell_L(X))$.

The proof of the following theorem can be found in Appendix A.

Theorem 2. *Let ℓ_1, \dots, ℓ_L be positively homogeneous and uniformly continuous functionals on $C(S)$. Further, assume that (3) and (6) hold. If $\xi \leq 0$, the spectral functions W belonging to the process Z in (3) are assumed to be strictly positive. Then, for $\xi \neq 0$ and $\xi x_1, \dots, \xi x_L > 0$,*

$$\lim_{t \rightarrow \infty} t \, \text{pr} \left[\exists j \in \{1, \dots, L\} : \frac{\ell_j(X)}{a(t)\ell_j\{A(s)\}} > x_j \right] = E \left(\bigvee_{j=1}^L \left[\frac{\ell_j\{W(s)^\xi A(s)\}}{|x_j|\ell_j\{A(s)\}} \right]^{1/\xi} \right). \quad (13)$$

For $\xi = 0$, we further require that (7) holds and that the functionals ℓ_j , $j = 1, \dots, L$, are linear. In this case, for any $x_1, \dots, x_L \in \mathbb{R}$,

$$\lim_{t \rightarrow \infty} t \, \text{pr} \left[\exists j \in \{1, \dots, L\} : \frac{\ell_j(X) - \ell_j\{b_s(t)\}}{a(t)\ell_j\{A(s)\}} > x_j \right] = E \left(\bigvee_{j=1}^L \exp \left[-x_j + \frac{\ell_j\{\log[W(s)]A(s)\}}{\ell_j\{A(s)\}} \right] \right). \quad (14)$$

The above theorem states that the vector $(\ell_1(X), \dots, \ell_L(X))$ of aggregations is in the max-domain of attraction of the multivariate max-stable distribution with exponent measure given by the right-hand side of (13) or (14), respectively. For the j th margin, for $\xi \neq 0$, the scale of the Weibull or Fréchet distribution is $\{\theta_\xi^{\ell_j}\}^\xi$, and for $\xi = 0$ the location parameter of the Gumbel distribution is $\log \theta_0^{\ell_j}$. This recovers the univariate results in Theorem 1. For details on multivariate domains of attraction and exponent measures, see Resnick [2008, Chapter 5]. In general this max-stable distribution will not be available in closed form, but for the purpose of evaluating risk regions for $(\ell_1(X), \dots, \ell_L(X))$, the exponent measure can be approximated by Monte Carlo methods. In the following important special case, we can compute the multivariate distribution explicitly.

EXAMPLE 7. *Consider the same framework as in Example 6, namely $S \subset \mathbb{R}^d$ compact, $\xi = 0$ and X is in the max-domain of attraction of Brown–Resnick process with spectral functions W . Suppose that for all $j = 1, \dots, L$, the functional ℓ_j is the spatial average over the compact region $A_j \subset S$, respectively. Since W is log-Gaussian in this case, the random vector*

$$(\ell_1\{\log[W(s)]A(s)\}/\ell_1\{A(s)\}, \dots, \ell_L\{\log[W(s)]A(s)\}/\ell_L\{A(s)\}), \quad (15)$$

is multivariate Gaussian, and its variogram matrix $\Gamma \in \mathbb{R}^{L \times L}$ can be computed explicitly; see Appendix B. The exponent measure in (14) therefore corresponds to a L -variate Hüsler–Reiss distribution with dependence matrix Γ whose j th margin has a Gumbel distribution with location parameter $\log \theta_0^{\ell_j}$ given in (12).

3 Statistical Inference

3.1 Setting

We suppose that we observe independent data X_1, \dots, X_n , $n \in \mathbb{N}$, from the process $X = \{X(s) : s \in S\}$, but only through the aggregation functionals ℓ_j satisfying the conditions from Theorem 2. The observations are therefore L -dimensional and of the form

$$(\ell_1(X_i), \dots, \ell_L(X_i)), \quad i = 1, \dots, n.$$

Making use of the limit results in Theorems 1 and 2, we aim to infer the extremal behavior of the whole process from the observed aggregated data. This requires estimation of both the marginal tail behavior and the extremal dependence of X . Naturally, further assumptions are needed to render this problem well-defined.

We suppose that the process X is in the functional max-domain of attraction of a max-stable process Z as in (3) with marginal distributions of $Z(s)$ of the form (4) for all $s \in S$. A natural and fairly general assumption on the marginal distributions of X is to belong to a location-scale family, i.e., for some distribution function F and continuous $A : S \rightarrow (0, \infty)$, $B : S \rightarrow \mathbb{R}$,

$$\text{pr}\{X(s) \leq x\} = F\left\{\frac{x - B(s)}{A(s)}\right\},$$

for any fixed $s \in S$. Since $X(s)$ is in the max-domain of attraction of $Z(s)$, the distribution of $M_n(s)$ must converge to G_ξ as $n \rightarrow \infty$. In particular, F must satisfy $\lim_{t \rightarrow \infty} F^t\{a(t)x + b(t)\} = G_\xi(x)$ for all $x \in \mathbb{R}$ with $\xi x \geq 0$ and appropriate functions $a : (0, \infty) \rightarrow (0, \infty)$ and $b : (0, \infty) \rightarrow \mathbb{R}$. This implies that the normalizing functions a_s and b_s of $X(s)$ can be chosen as

$$a_s(t) = A(s)a(t), \quad b_s(t) = B(s) + A(s)b(t), \quad t \in \mathbb{R}. \quad (16)$$

Moreover, if $\xi \neq 0$, without loss of generality, we may assume $B(s) \equiv 0$ by the same arguments as in the proof of Theorem 2.

We impose a parametric structure on the marginal scale and location parameters, i.e., the unknown functions A and B , respectively, and the extremal dependence of X , which is given by the exponent measure of Z . For the marginal distributions, we assume that A and B belong to parametric families of functions $\{A_{\vartheta_A}, \vartheta_A \in \Theta_A\}$ and $\{B_{\vartheta_B}, \vartheta_B \in \Theta_B\}$ where Θ_A and Θ_B are appropriate subsets of \mathbb{R}^{k_A} and \mathbb{R}^{k_B} , respectively. For the dependence, we suppose that the probability measure $\mathbb{P}^{(spec)}$ induced by the spectral function W of the limiting max-stable process Z belongs to a parametric class $\{\mathbb{P}_{\vartheta_W}^{(spec)}, \vartheta_W \in \Theta_W\}$ with $\Theta_W \subset \mathbb{R}^{k_W}$. Further, the joint normalization constants $a(t) \in (0, \infty)$ and $b(t) \in \mathbb{R}$ need to be estimated for some large t .

In the following, we present two ways to estimate the complete parameter vector

$$\vartheta = (a(t), b(t), \vartheta_A, \vartheta_B, \vartheta_W) \in (0, \infty) \times \mathbb{R} \times \Theta_A \times \Theta_B \times \Theta_W,$$

based on the marginal and multivariate tail behavior of $(\ell_1(X), \dots, \ell_L(X))$ as given in Theorems 1 and 2, respectively.

3.2 Least squares fit based on marginal estimates

Throughout the rest of this section, for the sake of simplicity we assume that $\xi = 0$ is known. Estimation for the case that ξ is unknown can be performed analogously, see Appendix C.

As a first approach, we approximate the tail of the distribution of $\ell_j(X)$ separately for each $j = 1, \dots, L$. From (14), we obtain for exceedances over sufficiently large $x \in \mathbb{R}$ and $t > 0$,

$$\text{pr} \{ \ell_j(X) > x \} \approx t^{-1} \exp \left(-\frac{x - \mu_{j,t}}{\sigma_{j,t}} \right), \quad (17)$$

or, equivalently, for block maxima,

$$[\text{pr} \{ \ell_j(X) \leq x \}]^t \approx \exp \left\{ -\exp \left(-\frac{x - \mu_{j,t}}{\sigma_{j,t}} \right) \right\}, \quad (18)$$

where the location parameters $\mu_{j,t}$ and the scale parameters $\sigma_{j,t}$, $j = 1, \dots, L$, are given by

$$\mu_{j,t}(\vartheta) = \ell_j \{ A_{\vartheta_A}(s) \} \cdot \left\{ b(t) + a(t) \log \theta_0^{\ell_j}(\vartheta) \right\} + \ell_j \{ B_{\vartheta_B}(s) \}, \quad (19)$$

$$\sigma_{j,t}(\vartheta) = a(t) \cdot \ell_j \{ A_{\vartheta_A}(s) \}, \quad (20)$$

respectively. While the asymptotic behavior of $\mu_{j,t}$ and $\sigma_{j,t}$ is uniquely determined by Equation (17), additional assumptions on $A(s)$ and $B(s)$, such as $\ell_1 \{ A(s) \} = 1$ and $\ell_1 \{ B(s) \} = 0$, are necessary to ensure the identifiability of a, b, A, B and $\theta_0^{\ell_j}$ from Equations (19) and (20).

For large t , estimates $\hat{\mu}_{j,t}$ and $\hat{\sigma}_{j,t}$ for $\mu_{j,t}$ and $\sigma_{j,t}$ can be obtained using well-known techniques from univariate extreme value statistics based on peaks-over-threshold or block maxima approaches, for instance. Here, the value of t is typically closely related to the choice of the threshold and the block size, respectively; see Appendix C for details. Based on these estimates, we define a weighted least squares estimator

$$\hat{\vartheta}_{\text{LS}} = \underset{\vartheta}{\text{argmin}} \sum_{j=1}^L v_j \cdot \{ \hat{\mu}_{j,t} - \mu_{j,t}(\vartheta) \}^2 + w_j \cdot \{ \hat{\sigma}_{j,t} - \sigma_{j,t}(\vartheta) \}^2,$$

where $v_j, w_j \geq 0$, $j = 1, \dots, L$, are appropriate weights and $\mu_{j,t}(\vartheta)$ and $\sigma_{j,t}(\vartheta)$ are given by Equations (19) and (20), respectively. A possible choice for $1/v_j$ and $1/w_j$ are the variances of the estimators $\hat{\mu}_{j,t}$ and $\hat{\sigma}_{j,t}$.

3.3 Censored likelihood for the joint tail behavior

Alternatively, we can estimate ϑ making use of the multivariate tail behavior of the whole vector $(\ell_1(X), \dots, \ell_L(X))$. For sufficiently large $x_1, \dots, x_L \in \mathbb{R}$ and $t > 0$, by Theorem 2,

$$\text{pr} \left\{ \exists j \in \{1, \dots, L\} : \frac{\ell_j(X) - \mu_{j,t}}{\sigma_{j,t}} > x_j \right\} \approx t^{-1} V_{\vartheta}(x_1, \dots, x_L),$$

where

$$V_{\vartheta}(x_1, \dots, x_L) = E_{\vartheta_W} \left(\max_{j=1}^L \exp \left[-x_j - \log \{ \theta_0^{\ell_j}(\vartheta) \} + \frac{\ell_j \{ \log[W(s)] A_{\vartheta_A}(s) \}}{\ell_j \{ A_{\vartheta_A}(s) \}} \right] \right), \quad (21)$$

is the exponent measure of a max-stable vector with standard Gumbel margins. Thus, the parameter vector ϑ can be estimated by a censored likelihood approach. Define a vector $u = (u_1, \dots, u_L)$ whose

j th element $u_j \in \mathbb{R}$ is a suitably high marginal threshold for $\ell_j(X)$, such as its empirical $(1 - 1/t)$ -quantile, and let $\mathcal{K}_i = \{j = 1, \dots, L : \ell_j(X_i) > u_j\}$. Denoting the normalized thresholds and data by $\tilde{u} = (\tilde{u}_1, \dots, \tilde{u}_L)$ and $Y_i = (Y_{i1}, \dots, Y_{iL})$ with

$$\tilde{u}_j = \frac{u_j - \mu_{j,t}}{\sigma_{j,t}}, \quad Y_{ij} = \frac{\ell_j(X_i) - \mu_{j,t}}{\sigma_{j,t}}, \quad j = 1, \dots, L,$$

respectively, we let $\hat{\vartheta}_{\text{cens}}$ be the argmax of the log-likelihood

$$(n - |\mathcal{I}|) \log \left\{ 1 - \frac{1}{t} V_{\vartheta}(\tilde{u}) \right\} + \sum_{i \in \mathcal{I}} \log \left(\left[\prod_{j \in \mathcal{K}_i} \frac{1}{a(t) \cdot \ell_j\{A_{\vartheta_A}(s)\}} \right] \cdot (-1) \cdot \frac{1}{t} V_{\vartheta, \mathcal{K}_i}(Y_i) \right), \quad (22)$$

where $\mathcal{I} = \{i = 1, \dots, n : \ell_j(X_i) > u_j \text{ with } j = 1, \dots, L\}$ and $V_{\vartheta, \mathcal{K}_i}$ are the partial derivatives of V_{ϑ} in directions \mathcal{K}_i . By the homogeneity of V_{ϑ} , it can be seen that the likelihood (22) asymptotically does not depend on the specific choice of t , but only on the u_1, \dots, u_L . This likelihood corresponds to multivariate threshold exceedances and their approximation by Pareto processes [cf., Thibaud and Opitz, 2015]. The censoring of the exponent measure V_{ϑ} reduces possible bias for observations below the marginal threshold that might not yet have converged to the limit model; see Wadsworth and Tawn [2014].

4 Simulation of Extreme Events

Environmental risk assessment is often based on rare event simulation of scenarios with long return periods. Two kinds of simulations are typically required: unconditional simulations of a given or fitted model capturing the spatial extent and the variability of possible extreme events; and simulations at points of interest conditional on a particular event that was only observed at different locations or scales. Conditional and unconditional simulations have for instance been studied for max-stable processes [Dombry et al., 2013, 2016] and for threshold exceedances [Thibaud and Opitz, 2015, de Fondeville and Davison, 2017]. In this section, we discuss how the multivariate result in Theorem 2 allows us to perform these two kinds of simulations for extreme events of the process X . We assume that the process X satisfies the assumptions of Theorem 2 for known normalizing functions a_s and b_s with representation (16), extreme value index $\xi \in \mathbb{R}$, and known distribution of the spectral process W . For simplicity, we again restrict to the case $\xi = 0$, but the procedure can be adapted for the case $\xi \neq 0$.

In order to simulate X at a finite number of locations $s_1, \dots, s_K \in S$, we artificially augment the vector of functionals to $(\ell_1(X), \dots, \ell_L(X), \ell_{L+1}(X), \dots, \ell_{L+K}(X))$, where $\ell_{L+k}(X) = X(s_k)$ is the point evaluation at location s_k , $k = 1, \dots, K$. We apply Theorem 2 to this augmented vector to obtain

$$\lim_{t \rightarrow \infty} t \, \text{pr} \left[\exists j \in \{1, \dots, L + K\} : \frac{\ell_j(X) - \mu_{j,t}}{\sigma_{j,t}} > x_j \right] = E \left\{ \bigvee_{j=1}^{L+K} \exp(-x_j + \log \Psi_j) \right\},$$

where

$$\Psi_j = \exp \left[\frac{\ell_j\{\log[W(s)]A(s)\}}{\ell_j\{A(s)\}} - \log \theta_0^{\ell_j} \right], \quad j = 1, \dots, L + K,$$

and $\mu_{j,t}$ and $\sigma_{j,t}$, $j = 1, \dots, L + K$, $t > 0$, are defined as in Equations (19) and (20), respectively. In other words, $(\ell_1(X), \dots, \ell_{L+K}(X))$ is in the-max-domain of attraction of a max-stable distribution with standard Gumbel margins and spectral vector $(\Psi_1, \dots, \Psi_{L+K})$.

In the framework of conditional simulation of an extreme event, the aggregated data $\ell_1(X) = y_1, \dots, \ell_L(X) = y_L$, are observed and one of them, say $\ell_J(X)$, is assumed to be large. Reformulating Theorem 2 in terms

of threshold exceedances, we obtain the convergence in distribution

$$\mathcal{L} \left[\left\{ \frac{\ell_j(X) - \mu_{j,t}}{\sigma_{j,t}} \right\}_{j=1}^{L+K} \mid \frac{\ell_J(X) - \mu_{J,t}}{\sigma_{J,t}} > 0 \right] \longrightarrow \mathcal{L}(U + \log \Psi^{(J)}), \quad (23)$$

as $t \rightarrow \infty$, where U is a standard exponential random variable and, independently of U , $\Psi^{(J)}$ is a $(L + K)$ -dimensional random vector with the transformed distribution P_J given in Dombry et al. [2016, Proposition 1]. For most popular models in spatial extremes, P_J can be simulated easily. Using approximation (23) with $u = (y_J - \mu_{J,t})/\sigma_{J,t} > 0$ for some large t , we can perform conditional simulation of the vector $(X(s_1), \dots, X(s_K))$ in the following way.

- (i) Simulate a realization $(\psi_{L+1}, \dots, \psi_{L+K})$ of the conditional distribution of $(\Psi_{L+1}^{(J)}, \dots, \Psi_{L+K}^{(J)})$ given that $\log \Psi_j^{(J)} = (y_j - \mu_{j,t})/\sigma_{j,t} - u$, $j = 1, \dots, L$.
- (ii) As a conditional realization of $(X(s_1), \dots, X(s_K))$, return $x = (x(s_1), \dots, x(s_K))$ with

$$x(s_k) = a_s(t) \cdot (u + \log \psi_{L+k}) + b_s(t), \quad k = 1, \dots, K. \quad (24)$$

For unconditional simulation, one is typically interested in extreme events in the sense that at least one of the functionals $\ell_1(X), \dots, \ell_L(X)$ exceeds a high threshold. Therefore, we replace the conditioning event in (23) by $\max_{j=1, \dots, L} \{\ell_j(X) - \mu_{j,t}\}/\sigma_{j,t} > 0$, such that the vector $\Psi^{(J)}$ in the limiting law in (23) becomes a vector $\Psi^{(\max)}$ that is normalized with respect to the maximum of its first L components [cf., Dombry and Ribatet, 2015]. Noting that $\Psi^{(\max)}$ can be generated by rejection sampling [cf., de Fondeville and Davison, 2017], we can adapt the conditional simulation procedure to obtain an unconditional extreme sample. Indeed, it suffices to let $(\psi_1, \dots, \psi_{L+K})$ in (i) be a realization of the unconditional distribution of $\Psi^{(\max)}$, and to replace the constant u in Equation (24) in (ii) by a realization of the standard exponential distribution U .

In order to perform conditional and unconditional simulation, the multivariate tail behavior of the vector $\ell(X)$ in the sense of Theorem 2 is required. For our running example of a limiting Brown–Resnick process, the following makes this explicit.

EXAMPLE 8. *As in Example 7, let $S \subset \mathbb{R}^d$ be compact, $\xi = 0$ and X is in the max-domain of attraction of a Brown–Resnick process. The aggregation functionals ℓ_j are spatial averages over compact regions $S_j \subset S$, $j = 1, \dots, L$, or point evaluations $\ell_{L+k}(X) = X(s_k)$ at locations $s_k \in S$, $k = 1, \dots, K$. The vector $(\ell_1(X), \dots, \ell_{L+K}(X))$ then satisfies the assumptions of Theorem 2, and it is in the max-domain of attraction of a multivariate Hüsler–Reiss distribution with dependence matrix*

$$\Gamma = \begin{pmatrix} \{\Gamma_{jk}\}_{j,k} & \{\Gamma_{jq}\}_{j,q} \\ \{\Gamma_{pk}\}_{p,k} & \{\Gamma_{pq}\}_{p,q} \end{pmatrix}, \quad \begin{cases} j, k = 1, \dots, L, \\ p, q = L+1, \dots, L+K. \end{cases}$$

The entries of the four sub-matrices and the explicit form of the exponent measure are given in Appendix B. In this case, the above algorithms essentially reduce to conditional and unconditional simulation of Gaussian processes.

5 Application: downscaling extremes

5.1 Statistical downscaling

Environmental data can be classified into two broad categories. On the one hand, station measurements are obtained through direct observation of the physical quantity. This type of data refers to a precise

location in space, but it may suffer from inhomogeneities between stations due to varying record lengths and differences between measurement instruments, and, moreover, it usually has a sparse spatial coverage. Gridded databases, for instance generated by climate models, on the other hand, cover a large region or even the entire globe, but at a coarse scale where data points can be considered as an aggregation of the physical variable.

Understanding the link from these gridded data to point measurements is an important area of research in environmental sciences called downscaling. Besides dynamical downscaling procedures based on the solution of partial differential equations describing the physical processes, a large number of downscaling techniques relying on the statistical relationship between variables at different scales have been applied. Most of these techniques focus on central characteristics of the distribution such as mean and variance. In geostatistics, for instance, the so-called change of support has been extensively studied for Gaussian processes [cf., Chiles and Delfiner, 2012, and references therein]. There are only few examples of statistical downscaling procedures for extremes. Mannshardt-Shamseldin et al. [2010] and Kallache et al. [2011] follow an approach related to univariate extreme value theory, and Bechler et al. [2015] and Oesting et al. [2017] propose conditional simulation from a spatial max-stable process that has been estimated from station measurements.

Here, using the theoretical results in Section 2, we extend the idea of changing the support of a stochastic process X to the context of extremes, basing inference only on aggregated observations $\ell_1(X), \dots, \ell_L(X)$. These might come from gridded data sets, as in our case, supposing that the grid values represent an aggregation of the underlying physical quantity. If additional station measurements $X(s_1), \dots, X(s_K)$ are available, they can also be used. Outputs of the method will be return level estimates at point locations, as well as unconditional and conditional simulations of rare events in the region S . The method allows for the estimation of marginal characteristics such as return levels at point locations, as well as unconditional and conditional simulations of rare events on the entire region S .

5.2 Application to extreme temperature in the South of France

We apply our downscaling procedure to daily temperature maxima in Europe from the e-obs data set [Haylock et al., 2008], which covers the period from 1950 to 2016 with a 0.25° grid resolution. To avoid potential temporal non-stationarity, we restrict the study to the summer period, i.e., July and August. Our study region S is a $80\text{km} \times 80\text{km}$ subset of the gridded product located in the south of France, in the west of Perpignan; see Figure 1. The region is mountainous and thus altitude appears to be a natural covariate for our model. The underlying spatial process of temperatures is denoted by $\{X(s) : s \in S\}$, and the observations $(\ell_1(X_i), \dots, \ell_L(X_i))$ on day i can be considered as the spatial averages over the $L = 12$ cells in S , where $i = 1, \dots, n$, and n is the number of days in the given time span of 67 years. The null hypothesis that the marginal tails of the aggregated data are in the Gumbel domain of attraction cannot be rejected, and we thus assume in sequel that $\xi = 0$.

Throughout we assume the same setting as in Section 3.1, namely that the marginal distributions of $X(s)$ belong to a location-scale family for all $s \in S$ parameterized through the functions

$$A(s) = 1, \quad B_{\vartheta_B}(s) = b_0 + b_1 \times \text{alt}(s) + b_2 \times \text{lon}(s) + b_3 \times \text{lat}(s),$$

where $\text{alt}(s)$, $\text{lon}(s)$ and $\text{lat}(s)$ denote the altitude, longitude and latitude at location $s \in S$, respectively. We further suppose that X is in the functional max-domain of attraction of a max-stable process Z belonging to a parametric family $\{Z_{\vartheta_W} : \vartheta_W \in \Theta_W\}$, for which we consider the Brown–Resnick processes introduced in Example 1, parameterized by $\vartheta_W = (\alpha, \lambda, \eta, a)$ for the anisotropic power variogram

$$\gamma(s_1, s_2) = \left\| \frac{\Omega(s_1 - s_2)}{\lambda} \right\|^\alpha, \quad s_1, s_2 \in S,$$

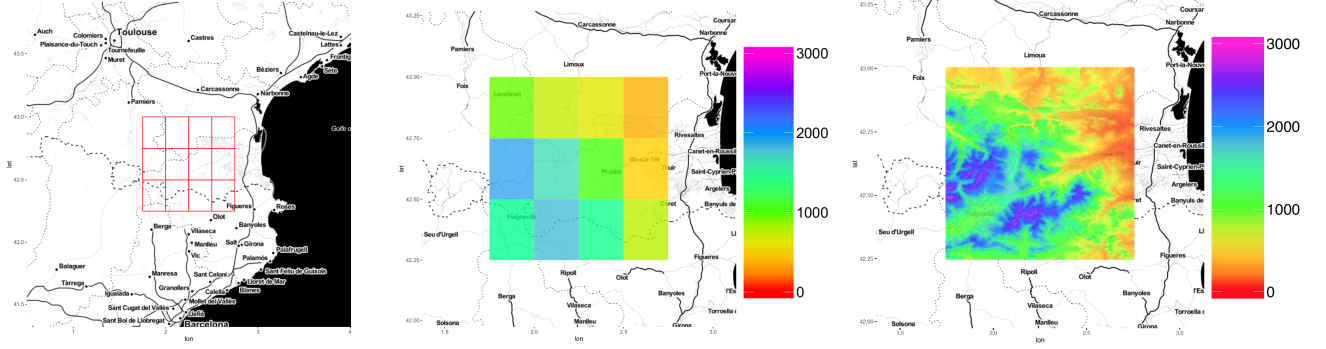


Figure 1: The study region consisting of 12 grid cells in the south of France (left), mean altitude within each cell (middle) and elevation in the region.

	a_n	b_n	b_1	b_2	b_3	α	λ	η	a
Estimate	1.90	35.53	4.51	-0.53	-0.20	0.90	6.42	-0.08	1.14
Standard deviation	0.06	0.27	0.14	0.26	0.28	0.07	0.51	0.22	0.08

Table 1: Estimated parameters and standard deviations for the temperature downscaling model. Standard deviations are computed using a block jackknife with 19 blocks of size 6.

with $0 < \alpha \leq 2$, $\lambda > 0$ and anisotropy matrix

$$\Omega = \begin{bmatrix} \cos \eta & -\sin \eta \\ a \sin \eta & a \cos \eta \end{bmatrix}, \quad \eta \in \left(-\frac{\pi}{2}; \frac{\pi}{2}\right], \quad a > 1.$$

In Sections 3.2 and 3.3 we discussed two approaches to estimate the parameters of this model, namely least squares estimation based on univariate location and scale estimates, and censored likelihood estimation for multivariate threshold exceedances. The formulas required for the implementation of these approaches have been derived in Sections 2 and 3 and in Appendix B. For least squares estimation, this includes the explicit expression (12) for the univariate ℓ -extremal coefficient. For censored likelihood estimation of the model parameters in (22), we require the partial derivatives V_K of the exponent measure V , which can be obtained as in Asadi et al. [2015, Section 4.3.2]; see Appendix B for more details. In order to assess the effectiveness and to compare the efficiency of the two methods, in Appendix D we perform a simulation study with a setup similar to this application. It turns out that the censored likelihood approach is significantly more efficient since it uses the full information on extremal dependence. The parameters of our model for temperature extremes are therefore fitted using the censored likelihood procedure based on all observations where at least one component exceeds its respective empirical 0.98 quantile. To avoid possible temporal dependence we keep only observations that are at least 5 days apart, yielding a set of 114 events. The parameter estimates are displayed in Table 1 where standard deviations are obtained using a jackknife procedure with 19 blocks of size 6; censored maximum likelihood is performed repeatedly with one block left out.

We assess the model fit in the diagnostic plots shown in Appendix E. First, we check the marginal distributions implied by the fitted linear model by comparing them in quantile-quantile plots to the observations; see Figure A1. The model provides a good fit for most stations and the quantiles of the fitted model generally remain in the confidence bounds obtained by parametric bootstrap. For a small number of stations, the model slightly over-estimates return levels.

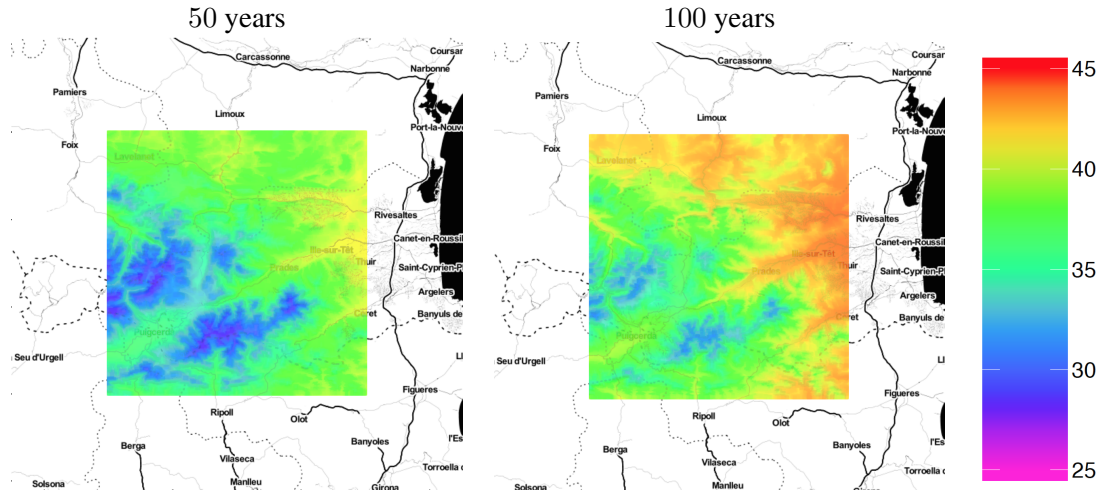


Figure 2: Downscaled return levels of daily temperature maxima ($^{\circ}\text{C}$) for the 50 (left) and 100 (right) years return periods in the south of France at a $25 \times 25\text{m}$ resolution.

Verification of the dependence structure is based on a graphical comparison of the pairwise extremogram [Davis and Mikosch, 2009] from the fitted multivariate Hüsler–Reiss model to its empirical counterpart based on the gridded observations. The extremogram values were significantly larger than zero for increasing thresholds and stable around the empirical 0.98 quantile, validating the asymptotic dependence model. Figure A2 shows that the fitted variogram model successfully captures the major trend of the cloud of points. The effect of spatial anisotropy seems to be rather weak, which is also reflected in the parameter estimate for a close to 1.

The fitted marginal model allows us to obtain return level maps for point locations at arbitrarily fine resolutions. In Figure 2, we produced such maps for the 50 and 100 year return periods. The full fitted model of marginal distributions and dependence structure further enables us to conditionally and unconditionally generate spatial extreme events of temperature fields at both a coarse and a fine resolution grid via the simulation procedures described in Section 4. Figure 3, for instance, displays two high resolution simulations of the temperature field conditionally on the observed aggregated temperatures during the warmest day of the 2003 heatwave. The simulations show that extreme temperatures at fine resolutions can be remarkably larger than at a coarse scale. Moreover, both simulations are constrained to have the same observed averages on the grid boxes, but they may exhibit different spatial patterns. This illustrates the variability of such a heatwave and provides practitioners with a set of possible scenarios that can be used for risk assessment.

Acknowledgement

We would like to thank Anthony C. Davison for helpful comments and discussions, and the Swiss National Science Foundation for financial support.

References

- P. Asadi, A. C. Davison, and S. Engelke. Extremes on river networks. *Ann. Appl. Stat.*, 9(1):2023–2050, 2015.

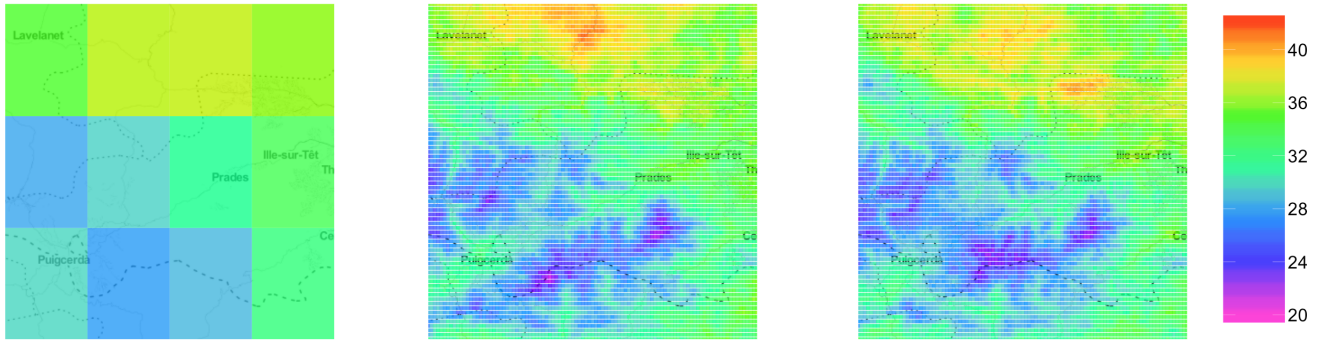


Figure 3: Maximal temperature ($^{\circ}\text{C}$) on the warmest day during the 2003 heatwave. Gridded data from the e-obs database [Haylock et al., 2008] (left); conditional simulations with a 1×1 km resolution (center and right).

- A. Bechler, M. Vrac, and L. Bel. A spatial hybrid approach for downscaling of extreme precipitation fields. *J. Geophys. Res. Atmos.*, 120(10):4534–4550, 2015.
- B. M. Brown and S. I. Resnick. Extreme values of independent stochastic processes. *J. Appl. Probab.*, 14(4):732–739, 1977.
- T. A. Buishand, L. de Haan, and C. Zhou. On spatial extremes: with application to a rainfall problem. *Ann. Appl. Stat.*, 2(2):624–642, 2008.
- J.-P. Chiles and P. Delfiner. *Geostatistics: Modeling Spatial Uncertainty*. John Wiley & Sons, 2012.
- S. G. Coles and J. A. Tawn. Modelling extremes of the areal rainfall process. *J. R. Stat. Soc. Ser. B Stat. Methodol.*, 58(2):329–347, 1996.
- R. A. Davis and T. Mikosch. The extremogram: a correlogram for extreme events. *Bernoulli*, 15:977–1009, 2009.
- R. de Fondeville and A. C. Davison. High-dimensional peaks-over-threshold inference. Available from <https://arxiv.org/abs/1605.08558>, 2017.
- L. de Haan. A spectral representation for max-stable processes. *Ann. Probab.*, 12(4):1194–1204, 1984.
- L. de Haan and A. Ferreira. *Extreme Value Theory: An Introduction*. Springer, Berlin, 2006.
- C. Dombry and M. Ribatet. Functionnal regular variations, Pareto processes and peaks over threshold. *Stat. Interface.*, 8(1):9–15, 2015.
- C. Dombry, F. Eyi-Minko, and M. Ribatet. Conditional simulation of max-stable processes. *Biometrika*, 100(1):111–124, 2013.
- C. Dombry, S. Engelke, and M. Oesting. Exact simulation of max-stable processes. *Biometrika*, 103(2):303–317, 2016.
- S. Engelke, A. Malinowski, Z. Kabluchko, and M. Schlather. Estimation of Hüsler–Reiss distributions and Brown–Resnick processes. *J. R. Stat. Soc. Ser. B Stat. Methodol.*, 77(1):239–265, 2015.

- A. Ferreira, L. de Haan, and C. Zhou. Exceedance probability of the integral of a stochastic process. *J. Multivar. Anal.*, 105(1):241–257, 2012.
- E. Giné, M. Hahn, and P. Vatan. Max-infinitely divisible and max-stable sample continuous processes. *Probab. Th. Rel. Fields*, 87(2):139–165, 1990.
- M. R. Haylock, N. Hofstra, A. M. G. Klein Tank, E. J. Klok, P. D. Jones, and M. New. A european daily high-resolution gridded data set of surface temperature and precipitation for 1950-2006. *J. Geophys. Res. Atmos.*, 113(D20), 2008.
- J. Hüsler and R.-D. Reiss. Maxima of normal random vectors: between independence and complete dependence. *Statist. Probab. Lett.*, 7(4):283–286, 1989.
- Z. Kabluchko. Extremes of independent Gaussian processes. *Extremes*, 14(3):285–310, 2011.
- Z. Kabluchko, M. Schlather, and L. de Haan. Stationary max-stable fields associated to negative definite functions. *Ann. Probab.*, 37(5):2042–2065, 2009.
- M. Kallache, M. Vrac, P. Naveau, and P.-A. Michelangeli. Nonstationary probabilistic downscaling of extreme precipitation. *J. Geophys. Res.-Atmos.*, 116, 2011.
- G. Mainik and P. Embrechts. Diversification in heavy-tailed portfolios: properties and pitfalls. *Annals of Actuarial Science*, 7(1):26–45, 2013.
- E. C. Mannshardt-Shamseldin, R. L. Smith, S. R. Sain, L. O. Mearns, and D. Cooley. Downscaling extremes: a comparison of extreme value distributions in point-source and gridded precipitation data. *Ann. Appl. Stat.*, 4:484–502, 2010.
- M. Oesting and K. Strokorb. Efficient simulation of Brown–Resnick processes based on variance reduction of Gaussian processes. Available from <https://arxiv.org/abs/1709.06037>, 2017.
- M. Oesting, L. Bel, and C. Lantuéjoul. Sampling from a max-stable process conditional on a homogeneous functional with an application for downscaling climate data. *Scand. J. Stat.*, 2017. To appear.
- T. Opitz. Extremal t processes: elliptical domain of attraction and a spectral representation. *J. Multivariate Anal.*, 122(1):409–413, 2013.
- M. D. Penrose. Semi-min-stable processes. *Ann. Probab.*, 20(3):1450–1463, 1992.
- M. D. Powell and T. A. Reinhold. Tropical cyclone destructive potential by integrated kinetic energy. *Bull. Am. Meteorol. Soc.*, 88(4):513–526, 2007.
- S. I. Resnick. *Extreme Values, Regular Variation and Point Processes*. Springer, New York, 2008.
- M. Schlather. Models for stationary max-stable random fields. *Extremes*, 5(1):33–44, 2002.
- M. Schlather and J. A. Tawn. A dependence measure for multivariate and spatial extreme values: properties and inference. *Biometrika*, 90(1):139–156, 2003.
- E. Thibaud and T. Opitz. Efficient inference and simulation for elliptical Pareto processes. *Biometrika*, 102(2):855–870, 2015.
- E. Thibaud, J. Aalto, D. S. Cooley, A. C. Davison, and J. Heikkinen. Bayesian inference for the Brown–Resnick process, with an application to extreme low temperatures. *Ann. Appl. Stat.*, 10(4):2303–2324, 2016.

H. Wackernagel. *Multivariate Geostatistics*. Springer, New York, 2003.

J. L. Wadsworth and J. A. Tawn. Efficient inference for spatial extreme value processes associated to log-Gaussian random functions. *Biometrika*, 101(1):1–15, 2014.

C. Zhou. Dependence structure of risk factors and diversification effects. *Insurance Math. Econom.*, 46(3):531–540, 2010.

A Proof of Theorem 2

Proof. Condition (3) implies that the exponent measure ν of Z , defined by

$$\nu(E) = E \left(\int_0^\infty u^{-2} 1\{uW(s) \in E\} du \right), \quad E \in \mathcal{C}_+(S), \quad (25)$$

where $C_+(S)$ and $\mathcal{C}_+(S)$ denote the analogues to $C(S)$ and $\mathcal{C}(S)$ for non negative functions, verifies

$$\nu(E) = \begin{cases} \lim_{n \rightarrow \infty} n \Pr \left(\left\{ \left[\frac{X(s) - b_s(n)}{a_s(n)} \right]_+^{1/\xi}, s \in S \right\} \in E \right), & \xi \neq 0, \\ \lim_{n \rightarrow \infty} n \Pr \left(\left\{ \exp \left\{ \frac{X(s) - b_s(n)}{a_s(n)} \right\}, s \in S \right\} \in E \right), & \xi = 0. \end{cases} \quad (26)$$

Closely related to the spectral process W , the measure ν incorporates the extremal dependence structure of X .

For the Fréchet case, we note that, by Proposition 1.11 in Resnick [2008], $b_s(n) \equiv 0$ is a valid choice for the norming constant. Thus, Proposition 0.2 therein implies that the fraction $b_s(n)/a_s(n)$ converges to zero for every $s \in S$ as $n \rightarrow \infty$. By the results in Subsection 9.2 in de Haan and Ferreira [2006], the convergence is uniform on S . Further, the continuous function A is strictly positive and thus bounded away from zero on the compact set S . Hence, by (6), for any $\varepsilon > 0$, we have $|a(n)^{-1}a_s(n) - A(s)| < \varepsilon A(s)$ and $|b_s(n)/a_s(n)| < \varepsilon$ for all $s \in S$ and sufficiently large n . We thus obtain the uniform bound

$$\begin{aligned} \frac{X(s)}{a(n)} &= \frac{a_s(n)}{a(n)} \frac{X(s) - b_s(n)}{a_s(n)} + \frac{a_s(n)}{a(n)} \left(\frac{b_s(n)}{a_s(n)} \right) \\ &\geq (1 - \varepsilon)A(s) \left[\frac{X(s) - b_s(n)}{a_s(n)} \right]_+ - 2(1 + \varepsilon)A(s)\varepsilon, \end{aligned}$$

and analogously

$$\frac{X(s)}{a(n)} \leq (1 + \varepsilon)A(s) \left[\frac{X(s) - b_s(n)}{a_s(n)} \right]_+ + 2(1 + \varepsilon)A(s)\varepsilon.$$

Hence, for any realization of X and sufficiently large n , there exists $\Delta(X, n) \in [1 - \varepsilon, 1 + \varepsilon]$ such that

$$\sup_{s \in S} \left| \frac{X(s)}{a(n)} - \Delta(X, n) \cdot A(s) \cdot \left[\frac{X(s) - b_s(n)}{a_s(n)} \right]_+ \right| \leq 2(1 + \varepsilon)\varepsilon \cdot \sup_{s \in S} A(s).$$

As each ℓ_j , $j = 1, \dots, L$, is uniformly continuous, there exists a function $h : (0, \infty) \rightarrow (0, \infty)$, $\lim_{\varepsilon \searrow 0} h(\varepsilon) = 0$, such that $\sup_{j=1, \dots, L} |\ell_j(f) - \ell_j(g)| \leq h(\varepsilon)$ for all $f, g \in C_+(S)$ such that $\|f - g\|_\infty \leq 2(1 + \varepsilon)\varepsilon \|A\|_\infty$. The homogeneity of each ℓ_j then entails

$$\begin{aligned} \frac{\ell_j(X)}{a(n)} &\geq \Delta(X, n) \cdot \ell_j \left\{ \left[\frac{X(s) - b_s(n)}{a_s(n)} \right]_+ A(s) \right\} - h(\varepsilon) \\ &\geq (1 - \varepsilon) \cdot \ell_j \left\{ \left[\frac{X(s) - b_s(n)}{a_s(n)} \right]_+ A(s) \right\} - h(\varepsilon), \quad j = 1, \dots, L, \end{aligned}$$

and

$$\frac{\ell_j(X)}{a(n)} \leq (1 + \varepsilon) \cdot \ell_j \left\{ \left[\frac{X(s) - b_s(n)}{a_s(n)} \right]_+ A(s) \right\} + h(\varepsilon), \quad j = 1, \dots, L.$$

With $\varepsilon \searrow 0$, for $x_1, \dots, x_L > 0$, we obtain

$$\begin{aligned} & \lim_{n \rightarrow \infty} n \operatorname{pr} \left[\exists j \in \{1, \dots, L\} : \frac{\ell_j(X)}{a(n)} > x_j \right] \\ &= \lim_{n \rightarrow \infty} n \operatorname{pr} \left[\exists j \in \{1, \dots, L\} : \ell_j \left\{ \left[\frac{X(s) - b_s(n)}{a_s(n)} \right]_+ A(s) \right\} > x_j \right] \\ &= \lim_{n \rightarrow \infty} n \operatorname{pr} \left(\exists j \in \{1, \dots, L\} : \ell_j \left[\left\{ \left[\frac{X(s) - b_s(n)}{a_s(n)} \right]_+^{1/\xi} \right\}^\xi A(s) \right] > x_j \right) \\ &= \nu \left(\left\{ f \in C_+(S) : \exists j \in \{1, \dots, L\} \text{ with } \ell_j \left\{ f(s)^\xi A(s) \right\} > x_j \right\} \right) \\ &= E \left(\int_0^\infty u^{-2} 1_{\{\exists j \in \{1, \dots, L\} : \ell_j[\{uW(s)\}^\xi A(s)] > x_j\}} du \right) = E \left(\bigvee_{j=1}^L \left[\frac{\ell_j\{W(s)^\xi A(s)\}}{x_j} \right]^{1/\xi} \right), \end{aligned}$$

where we used (26) and (25). The proof for the Weibull case is analogous. In the Gumbel case, the integral in the proof of Theorem 2.1 in Ferreira et al. [2012] can just be replaced by the linear functionals ℓ_1, \dots, ℓ_L to obtain that

$$\begin{aligned} & \lim_{n \rightarrow \infty} n \operatorname{pr} \left[\exists j \in \{1, \dots, L\} : \frac{\ell_j(X) - \ell_j\{b_s(n)\}}{a(n)} > x_j \right] \\ &= \lim_{n \rightarrow \infty} n \operatorname{pr} \left[\exists j \in \{1, \dots, L\} : \ell_j \left\{ \frac{X(s) - b_s(n)}{a_s(n)} A(s) \right\} > x_j \right] \\ &= \lim_{n \rightarrow \infty} n \operatorname{pr} \left\{ \exists j \in \{1, \dots, L\} : \ell_j \left(\log \left[\exp \left\{ \frac{X(s) - b_s(n)}{a_s(n)} \right\} \right] A(s) \right) > x_j \right\} \\ &= \nu \{ f \in C_+(S) : \exists j \in \{1, \dots, L\} \text{ with } \ell_j[\log\{f(s)\}A(s)] > x_j \}, \end{aligned}$$

for $x_1, \dots, x_L \in \mathbb{R}$. Using its definition in (25), the exponent measure can be calculated yielding

$$\begin{aligned} & \nu \{ f \in C_+(S) : \exists j \in \{1, \dots, L\} \text{ with } \ell_j(\log(f(s))A(s)) > x_j \} \\ &= E \left(\int_0^\infty u^{-2} 1_{\left\{ \exists j \in \{1, \dots, L\} : \log u > \frac{x_j - \ell_j[\log\{W(s)\}A(s)]}{\ell_j\{A(s)\}} \right\}} du \right) \\ &= E \left\{ \bigvee_{j=1}^L \exp \left(\frac{x_j - \ell_j[\log\{W(s)\}A(s)]}{\ell_j\{A(s)\}} \right) \right\}. \end{aligned}$$

Replacing x_j by $x_j \cdot \ell_j\{A(s)\}$ closes the proof. \square

B Background and formulas related to Hüsler–Reiss distributions

B.1 Hüsler–Reiss distributions

The class of Brown–Resnick processes takes a similar role in spatial extreme value statistics as Gaussian processes in classical geostatistics. In order to specify their finite dimensional distributions, we recall a popular model in multivariate extreme value theory, namely the Hüsler–Reiss distribution [Hüsler and

Reiss, 1989]. An m -dimensional max-stable random vector (Z_1, \dots, Z_m) with distribution function $F_Z(x_1, \dots, x_m) = \exp\{-V(x_1, \dots, x_m)\}$ is Hüsler–Reiss distributed with Gumbel margins and strictly conditionally negative definite parameter matrix $\Gamma \in [0, \infty)^{m \times m}$ if its exponent measure has the form

$$V(x_1, \dots, x_m) = E \left[\max_{j=1, \dots, m} \exp \left\{ -x_j + Y_j - \frac{1}{2} \text{var}(Y_j) \right\} \right], \quad (27)$$

for a centered Gaussian random vector (Y_1, \dots, Y_m) with variogram matrix $\Gamma_{jk} = E\{(Y_j - Y_k)^2\}$, $1 \leq j, k \leq m$. In this case, one possible choice for the covariance matrix of Y is

$$\Sigma = \frac{1}{2} (\Gamma_{j1} + \Gamma_{k1} - \Gamma_{jk})_{1 \leq j, k \leq m}. \quad (28)$$

The exponent measure V is normalized in the sense that $V(\infty, \dots, x_j, \dots, \infty) = \exp(-x_j)$, for any $j = 1, \dots, m$. If Z is a Brown–Resnick process associated to the variogram γ , then the distribution of $(Z(s_1), \dots, Z(s_m))$ is Hüsler–Reiss with parameter matrix $\Gamma = \{\gamma(s_j, s_k)\}_{j, k=1, \dots, m}$.

For censored likelihood estimation (cf., Section 3.3) of models with Hüsler–Reiss limit, we require the partial derivatives $V_{\mathcal{K}}$ of V in (27) with respect to any non-empty subset of variables $\mathcal{K} \subset \{1, \dots, m\}$. Let $b \in \{1, \dots, m\}$ be the number of components that exceed their thresholds, and, without loss of generality, let $\mathcal{K} = \{1, \dots, b\}$. Based on the results in Engelke et al. [2015], Wadsworth and Tawn [2014] and Asadi et al. [2015, Section 4.3.2], we obtain the representation

$$(-1) \cdot V_{\mathcal{K}}(z) = \exp(-z_1) \varphi_{b-1}(\tilde{z}_{2:b}; \Sigma_{2:b}) \Phi_{L-b}\{\mu_C(z_{1:L}), \Sigma_C(z_{1:b})\}, \quad (29)$$

where $\tilde{z} = \{(z_j - z_1) + \Gamma_{1j}/2\}_{1 \leq j \leq m}$, Σ is as in (28) and $\varphi_k(\cdot, \Psi)$ and $\Phi_k(\cdot, \Psi)$ are the multivariate density and distribution function of a k -variate normal distribution with covariance Ψ . We use the convention that $\varphi_0 \equiv 1$ if $b = 1$ and $\Phi_0 \equiv 1$ if $b = m$, respectively. The mean μ_C and covariance matrix Σ_C are

$$\begin{aligned} \mu_C &= \tilde{z}_{(b+1):m} - \Sigma_{(b+1):m, 2:b} \Sigma_{2:b, 2:b}^{-1} \tilde{z}_{2:b}, \\ \Sigma_C &= \Sigma_{(b+1):m, (b+1):m} - \Sigma_{(b+1):m, 2:b} \Sigma_{2:b, 2:b}^{-1} \Sigma_{2:b, (b+1):m}. \end{aligned}$$

B.2 Explicit formulas for extremes of aggregated data

In the case where the underlying process X is in the domain of attraction of a Brown–Resnick process with Gumbel margins, we can obtain explicit formulas for the ℓ -extremal coefficient and the multivariate limits for certain aggregation functionals.

Throughout this section we work with the general assumptions and notations in Section 2, and concentrate on the case where $\xi = 0$ and the limiting process Z is a Brown–Resnick process on a compact region $S \subset \mathbb{R}^d$. We further assume that the variogram γ as defined in Example 1 depends on the spatial lag $s - t$ only and we therefore write $\gamma(s - t)$ for $\gamma(s, t)$. Then, without loss of generality, we may assume that $G(0) = 0$ and the spectral function simplifies to

$$W(s) = \exp \{G(s) - \gamma(s)/2\}, \quad s \in S.$$

We start with proving the closed form expression of the ℓ -extremal coefficient θ_0^{avg} , where ℓ is a spatial average over the region S ; see Example 6. Denoting $\bar{A} = \int_S A(s) \, ds$, it follows from Theorem 1 that

$$\theta_0^{\text{avg}} = E \left(\exp \left[\frac{1}{\bar{A}} \int_S \{G(s) - \gamma(s)/2\} A(s) \, ds \right] \right) = \exp \left\{ \frac{\sigma_{\text{avg}}^2}{2} - \frac{1}{2\bar{A}} \int_S A(s) \gamma(s) \, ds \right\}, \quad (30)$$

since the integral over a Gaussian process is normally distributed with variance

$$\sigma_{\text{avg}}^2 = \text{var} \left\{ \frac{\int_S A(s)G(s) \, ds}{\bar{A}} \right\} = \frac{1}{\bar{A}} \int_S A(s)\gamma(s) \, ds - \frac{1}{2\bar{A}^2} \int_S \int_S A(s)A(t)\gamma(s-t) \, ds \, dt,$$

which is a simple extension of Wackernagel [2003, p 67-69]. Plugging this into (30) yields formula (12). For censored likelihood inference in Section 3.3 and conditional or unconditional simulation described in Section 4, the multivariate limit behavior of different functions is required. We consider here the case that is used in the application, namely that the aggregation functionals are either spatial averages over compact regions $S_l \subset S$, $l = 1, \dots, L$, or point evaluations at locations $s_k \in S$, $k = 1, \dots, K$, i.e.,

$$\ell_j(X) = \begin{cases} \frac{1}{|S_j|} \int_{S_j} X(s) \, ds, & j = 1, \dots, L, \\ X(s_{j-L}), & j = L+1, \dots, L+K. \end{cases} \quad (31)$$

The vector $(\ell_1(X), \dots, \ell_{L+K}(X))$ then satisfies the assumptions of Theorem 2 and its limiting exponent measure \tilde{V} is the right-hand side of (14). This exponent measure is not normalized, since by Theorem 1, $\tilde{V}(\infty, \dots, x_j, \dots, \infty) = \exp(-x_j + \log \theta_0^{\ell_j})$, and $\log \theta_0^{\ell_j}$ is given by (12) for $j = 1, \dots, L$, and is equal to 0 for $j = L+1, \dots, L+K$. We therefore define the corresponding normalized exponent measure by

$$\begin{aligned} V(x_1, \dots, x_{L+K}) &= E \left\{ \max_{j=1, \dots, L+K} \exp \left(-x_j + \frac{\ell_j[\{G(s) - \gamma(s)/2\}A(s)]}{\ell_j\{A(s)\}} - \log \theta_0^{\ell_j} \right) \right\} \\ &= E \left\{ \max_{j=1, \dots, L+K} \exp \left(-x_j + \frac{\ell_j\{G(s)A(s)\}}{\ell_j\{A(s)\}} - \frac{1}{2} \text{var} \left[\frac{\ell_j\{G(s)A(s)\}}{\ell_j\{A(s)\}} \right] \right) \right\}, \end{aligned} \quad (32)$$

where the second equality follows from (30). Since all aggregation functionals are either spatial averages or point evaluations, and the vector (Y_1, \dots, Y_{L+K}) with $Y_j = \ell_j\{G(s)A(s)\}/\ell_j\{A(s)\}$, $j = 1, \dots, L+K$, is multivariate Gaussian, we recognize in (32) the exponent measure of a Hüsler–Reiss distribution with parameter matrix Γ where $\Gamma_{jk} = E(Y_j - Y_k)^2$, $j, k = 1, \dots, L+K$. We can separate Γ in different blocks such that

$$\Gamma = \begin{pmatrix} \{\Gamma_{jk}\}_{j,k} & \{\Gamma_{jq}\}_{j,q} \\ \{\Gamma_{pk}\}_{p,k} & \{\Gamma_{pq}\}_{p,q} \end{pmatrix}, \quad \begin{cases} j, k = 1, \dots, L, \\ p, q = L+1, \dots, L+K. \end{cases} \quad (33)$$

We directly see that $\Gamma_{pq} = \gamma(s_{p-L} - s_{q-L})$ for $p, q = L+1, \dots, L+K$. Since Γ is symmetric, letting $\bar{A}_j = \int_{S_j} A(s) \, ds$, $j = 1, \dots, L$, it suffices to compute

(i) for $j, k = 1, \dots, L$,

$$\begin{aligned} \Gamma_{jk} &= \frac{1}{\bar{A}_j \bar{A}_k} \int_{S_j} \int_{S_k} A(s)A(t)\gamma(s-t) \, ds \, dt - \frac{1}{2\bar{A}_j^2} \int_{S_j} \int_{S_j} A(s)A(t)\gamma(s-t) \, ds \, dt \\ &\quad - \frac{1}{2\bar{A}_k^2} \int_{S_k} \int_{S_k} A(s)A(t)\gamma(s-t) \, ds \, dt; \end{aligned}$$

(ii) for $j = 1, \dots, L$, $q = L+1, \dots, L+K$,

$$\Gamma_{jq} = \frac{1}{\bar{A}_j} \int_{S_j} A(s)\gamma(s - s_{q-L}) \, ds - \frac{1}{2\bar{A}_j^2} \int_{S_j} \int_{S_j} A(s)A(t)\gamma(s-t) \, ds \, dt.$$

In order to show (i), we note that for $s, t \in S$,

$$\text{var} \left\{ \frac{A(s)G(s)}{\bar{A}_j} - \frac{A(t)G(t)}{\bar{A}_k} \right\} = \frac{A(s)^2}{\bar{A}_j^2} \gamma(s) + \frac{A(t)^2}{\bar{A}_k^2} \gamma(t) - \frac{A(s)A(t)}{\bar{A}_j \bar{A}_k} \{\gamma(s) + \gamma(t) - \gamma(s-t)\}, \quad (34)$$

since $E\{G(s)^2\} = \gamma(s)$ and $E\{G(s)G(t)\} = 1/2 \{\gamma(s) + \gamma(t) - \gamma(s-t)\}$. We use the following [cf., Wackernagel, 2003, p 67-69]

$$\begin{aligned}\Gamma_{jk} &= \text{var} \left\{ \frac{1}{\bar{A}_j} \int_{S_j} A(s)G(s) \, ds - \frac{1}{\bar{A}_k} \int_{S_k} A(t)G(t) \, dt \right\} \\ &= \int_{S_j} \int_{S_k} \text{var} \left\{ \frac{A(s)G(s)}{\bar{A}_j} - \frac{A(t)G(t)}{\bar{A}_k} \right\} \, ds \, dt - \frac{1}{2} \int_{S_j} \int_{S_j} \text{var} \left\{ \frac{A(s)G(s)}{\bar{A}_j} - \frac{A(t)G(t)}{\bar{A}_j} \right\} \, ds \, dt \\ &\quad - \frac{1}{2} \int_{S_k} \int_{S_k} \text{var} \left\{ \frac{A(s)G(s)}{\bar{A}_k} - \frac{A(t)G(t)}{\bar{A}_k} \right\} \, ds \, dt.\end{aligned}\tag{35}$$

Using (34), the first term in the last equation equals

$$\begin{aligned}&\frac{|S_k|}{\bar{A}_j^2} \int_{S_j} A(s)^2 \gamma(s) \, ds + \frac{|S_j|}{\bar{A}_k^2} \int_{S_k} A(s)^2 \gamma(s) \, ds - \frac{|S_k|}{\bar{A}_j} \int_{S_j} A(s) \gamma(s) \, ds \\ &\quad - \frac{|S_k|}{\bar{A}_k} \int_{S_k} A(s) \gamma(s) \, ds + \frac{1}{\bar{A}_j \bar{A}_k} \int_{S_j} \int_{S_k} A(s) A(t) \gamma(s-t) \, ds \, dt.\end{aligned}$$

For the second term in (35), this simplifies to

$$\frac{2|S_j|}{\bar{A}_j^2} \int_{S_j} A(s)^2 \gamma(s) \, ds - \frac{2|S_j|}{\bar{A}_j} \int_{S_j} A(s) \gamma(s) \, ds + \frac{1}{\bar{A}_j^2} \int_{S_j} \int_{S_j} A(s) A(t) \gamma(s-t) \, ds \, dt,$$

and analogously for the third term. Putting this together, we obtain the formula in (i). Very similar calculations yield the result in (ii).

With the above calculation we have shown that the $(L + K)$ -dimensional vector in (31) is in the max-domain of attraction of a Hüsler–Reiss distribution with explicitly known parameter matrix, and we can use the inference and simulation methodology described in Sections 3 and 4 and in the literature.

C Estimation of the marginal normalizing constants $\mu_{j,n}$ and $\sigma_{j,n}$

We present two classical approaches to estimate the marginal location and scale parameters $\mu_{j,t}$ and $\sigma_{j,t}$ in Equations (19) and (20), respectively, for large t , namely the peaks over threshold approach based on Equation (17) and the block maxima approach based on (18). These approaches can be used in the first step of the least squares estimation procedure described in Section 3.2.

As a first approach, the parameters can be obtained by a censored likelihood approach for exceedances over high thresholds based on Equation (17). Let u_j be a suitably high marginal threshold, such as the empirical $(1 - 1/t)$ -quantile of $\ell_j(X)$, and $\mathcal{I} = \{i = 1, \dots, n : \ell_j(X_i) > u_j\}$. We then consider the censored log-likelihood

$$\log L_j^{(\text{cens})}(\mu_j, \sigma_j) \propto (n - |\mathcal{I}|) \cdot \left\{ 1 - \frac{1}{t} \exp \left(-\frac{u_j - \mu_j}{\sigma_j} \right) \right\} - |\mathcal{I}| \cdot \log(n\sigma_j) - \sum_{i \in \mathcal{I}} \frac{\ell_j(X_i) - \mu_j}{\sigma_j}$$

to obtain the estimate $(\hat{\mu}_{j,t}, \hat{\sigma}_{j,t}) = \arg\max_{\mu_j \in \mathbb{R}, \sigma_j > 0} \log L_j^{(\text{cens})}(\mu_j, \sigma_j)$.

As a second approach, we can estimate the parameters based on block maxima with a sufficiently large block size $t \in \mathbb{N}$, which, for simplicity, is assumed to satisfy $n = t \cdot n_t$ for some $n_t \in \mathbb{N}$. For the i.i.d. random variables $M_{t,k}^{(j)}$, $k = 1, \dots, n_t$, defined by

$$M_{t,k}^{(j)} = \max_{i=(k-1)t+1, \dots, kt} \ell_j(X_i),$$

we have

$$\text{pr} \left(M_{t,k}^{(j)} \leq x \right) = [\text{pr} \{ \ell_j(X) \leq x \}]^t \approx \exp \left\{ - \exp \left(- \frac{x - \mu_{j,t}}{\sigma_{j,t}} \right) \right\},$$

cf., Equation (18). Thus, we obtain estimates $(\hat{\mu}_{j,t}, \hat{\sigma}_{j,t}) = \text{argmax}_{\mu \in \mathbb{R}, \sigma > 0} \log L_j^{(\text{BM})}(\mu, \sigma)$ where

$$\log L_j^{(\text{BM})}(\mu, \sigma) = -n_t \cdot \log \sigma - \sum_{k=1}^{n_t} \left\{ \frac{M_{t,k}^{(j)} - \mu}{\sigma} + \exp \left(- \frac{M_{t,k}^{(j)} - \mu}{\sigma} \right) \right\}$$

is the Gumbel likelihood.

In order to have comparable estimates $\hat{\mu}_{j,t}$ and $\hat{\sigma}_{j,t}$ obtained for different values t_1 and t_2 , we can make use of the relationship $\left\{ \text{pr} \left(M_{t_1,k}^{(j)} \leq x \right) \right\}^{n/t_1} = \left\{ \text{pr} \left(M_{t_2,k}^{(j)} \leq x \right) \right\}^{n/t_2}$. Then, the approximation (18) by Gumbel distributions yields

$$\mu_{j,t_1} + \sigma_{j,t_1} \cdot \log(n/t_1) \approx \mu_{j,t_2} + \sigma_{j,t_2} \cdot \log(n/t_2) \quad \text{and} \quad \sigma_{j,t_1} \approx \sigma_{j,t_2} \quad (36)$$

for $t_1, t_2 \in \mathbb{R}$ being both sufficiently large. Thus, estimators $\hat{\mu}_{j,t_2}$ and $\hat{\sigma}_{j,t_2}$ can be obtained by plugging $\hat{\mu}_{j,t_1}$ and $\hat{\sigma}_{j,t_1}$ into relation (36).

REMARK 2. *Note that, in both cases, the estimators $\hat{\mu}_{j,t}$ and $\hat{\sigma}_{j,t}$ are obtained independently for each $j = 1, \dots, L$ via a maximum likelihood approach. Thus, the estimated vector $((\hat{\mu}_{j,t})_{j=1}^L, (\hat{\sigma}_{j,t})_{j=1}^L)$ also maximizes the independent log-likelihood functions*

$$\log L^{(\text{cens})} \{ (\mu_j)_{j=1}^L, (\sigma_j)_{j=1}^L \} = \sum_{j=1}^L \log L_j^{(\text{cens})}(\mu_j, \sigma_j)$$

and

$$\log L^{(\text{BM})} \{ (\mu_j)_{j=1}^L, (\sigma_j)_{j=1}^L \} = \sum_{j=1}^L \log L_j^{(\text{BM})}(\mu_j, \sigma_j),$$

respectively. Such an independent likelihood could also be used to estimate ξ if unknown.

D Simulation study

In this simulation study we apply our downscaling approach to a simple model that resembles the setup in the application in Section 5. We suppose that we observe independent data X_1, \dots, X_n from a process X on $S = [0, 5]^2$, but only through aggregating functionals ℓ_j , $j = 1, \dots, L$, with $L = 25$, which we will take to be spatial averages. The observations are thus 25-dimensional and of the form

$$\left(\frac{1}{|S_1|} \int_{S_1} X_i(s) \, ds, \dots, \frac{1}{|S_{25}|} \int_{S_{25}} X_i(s) \, ds \right), \quad i = 1, \dots, n,$$

where $S_j = [s_1^j, s_1^j + 1] \times [s_2^j, s_2^j + 1]$, with $s_1^j, s_2^j \in \{0, \dots, 4\}$, i.e., a regular grid of 1×1 squares. We consider X in the Gumbel ($\xi = 0$) max-domain of attraction of a Brown–Resnick process associated to the semi-variogram model

$$\gamma(s, t) = \left(\frac{\|s - t\|_2}{\lambda} \right)^\alpha, \quad \alpha = 1.5, \lambda = 1.$$

We impose a linear structure on the unknown functions A and B of the margins appearing in the setting described in Section 3.1,

$$\begin{aligned} A(s_1, s_2) &= a_0 + a_1 \times s_1 = 0.8 + 0.4 \times s_1, \\ B(s_1, s_2) &= b_0 + b_2 \times s_2 = -0.4 + 0.8 \times s_2, \end{aligned} \quad (s_1, s_2) \in [0, 5]^2,$$

where the parameters were chosen such that $\ell_1\{A(s)\} = 1$ and $\ell_1\{B(s)\} = 0$.

By Theorem 2 and Example 7, the vector of aggregated data $(\ell_1(X), \dots, \ell_L(X))$ is in the max-domain of attraction of a multivariate Hüsler–Reiss distribution with dependence matrix Γ described in Section B.2 and normalizing vectors $\{\mu_{j,t}\}_{j=1}^L$ and $\{\sigma_{j,t}\}_{j=1}^L$ as given in Equations (19) and (20), respectively. Such a vector of aggregated data can be simulated as follows.

1. Randomly select $j_0 \in \{1, \dots, 25\}$.
2. Generate a univariate exponential variable $U \sim \text{Exp}(1)$.
3. Generate a 24-dimensional Gaussian vector G with covariance matrix $\Sigma = (1/2)\{\Gamma_{jj_0} + \Gamma_{k j_0} - \Gamma_{jk}\}_{j,k \neq j_0}$ and mean $\mu = -\{\Gamma_{jj_0}/2\}_{j \neq j_0}$.
4. Set $\tilde{G}_{j_0} = 0$, $\tilde{G}_{-j_0} = G$ and $\tilde{Y} = \{U + \tilde{G} - \log \|\exp(\tilde{G})\|_1\} + \log 25$.
5. Set $Y_j = \ell_j(A)\{\tilde{Y}_j + \log \theta_0^{\ell_j}\} + \ell_j(B)$ for $j = 1, \dots, 25$.
6. Return $Y = (Y_1, \dots, Y_{25})$.

We simulate $n = 10^4$ samples Y_1, \dots, Y_n of the random vector Y , which are then used to estimate the model parameters via the least squares and censored likelihood procedures. Note that we could have simulated the process X on a fine grid and then aggregated it over the squares. This approach is computationally very inefficient and gives essentially the same results as those presented in the sequel.

For the least squares procedure, we use the block maxima approach grouping the 10000 replicates are into blocks of size 100 in which we compute the maxima, yielding theoretically $a(t) = 1$ and $b(t) = \log(100)$ for $t = 100$. We also compute spatial means for larger squares with side length 2, 3, 4, 5 and then estimate the scale and location parameters using the univariate estimator described in Section 3.2. The least squares fit is then performed based on the estimated scales and locations of the spatial means over the different squares.

For the censored likelihood method, we choose a threshold vector $u \in \mathbb{R}^L$, based on local empirical quantiles, such that the number N_u of observations $Y_i, i = 1, \dots, n$, with $\max(Y_{i1}/u_1, \dots, Y_{i25}/u_L) \geq 1$ equals 100. In other words, we keep the 100 highest exceedances. In this setting, we have $a(t) = 1$ and $b(t) = \log(10000)$ with $t = 10000$. Finally, we use these 100 exceedances in the censored likelihood procedure described by Equation (22).

The results in Table A2 show that all parameters can be estimated accurately. The censored likelihood approach, which makes use of the multivariate tail distribution, outperforms the least squares procedure, which relies only on marginal properties, by about 30%. The advantage would be even larger if we would use more than 100 exceedances, but we fixed this number to equal the number of block maxima.

	$a(t)$	a_0	a_1	$b(t)$	b_0	b_2	α	λ	Mean
Censored LLH	8.4	1.1	4.2	3.0	8.7	8.7	4.4	9.4	6.4
Least squares	7.6	2.7	11.4	6.6	7.7	7.7	5.3	10.2	8.1

Table A2: Relative root mean square error (%) for estimates based on censored likelihood and least squares procedures. Inference is performed based on the $n = 10^4$ simulated data above.

E Model Assessment

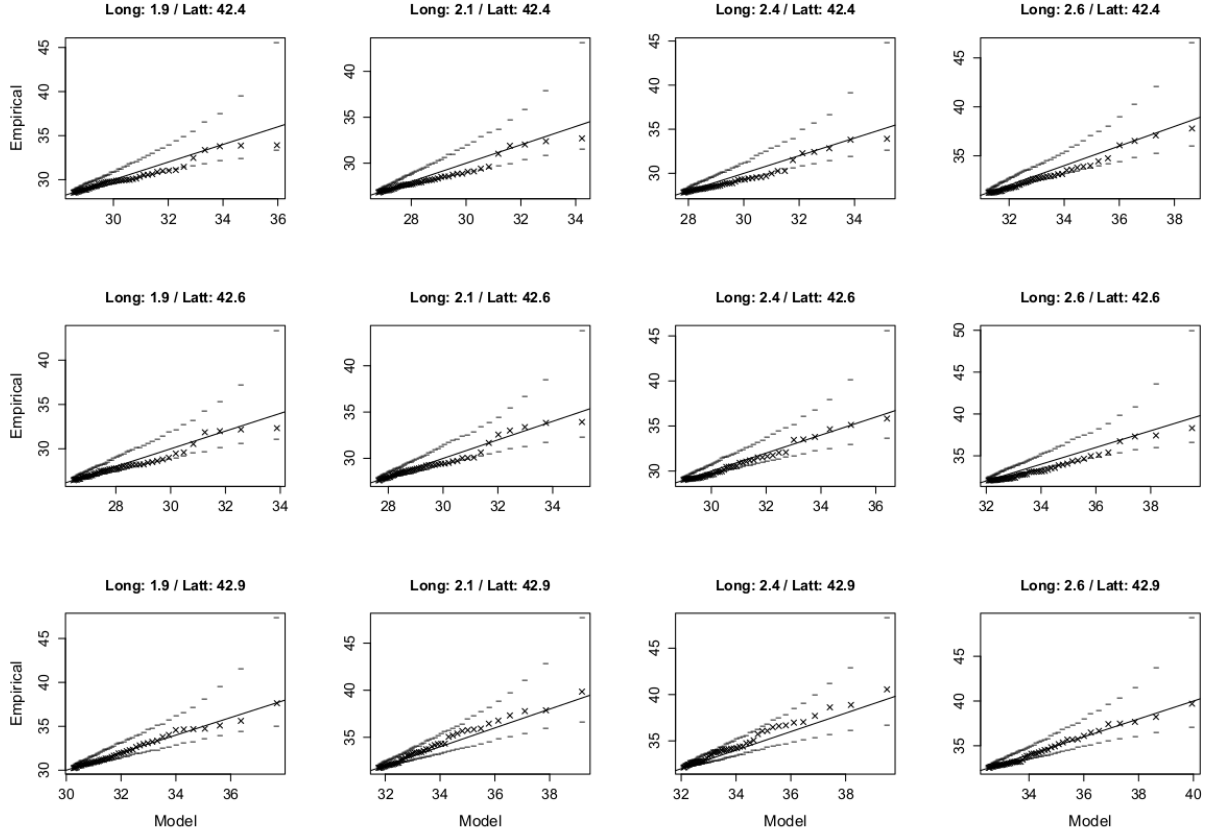


Figure A1: Quantile-quantile plots comparing the observations and the fitted marginal distribution for every grid cell. Pointwise confidence intervals are obtained by parametric bootstrap taking into account the uncertainty of the parameter estimates.

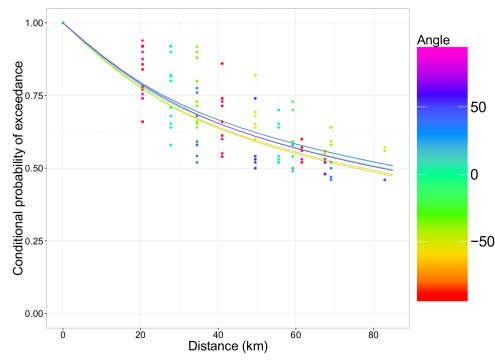


Figure A2: Estimated pairwise extremogram (dots) as function of the distance (km) between the centers of the grid cells and direction ($^{\circ}$). The solid lines represent the theoretical extremogram for the estimated anisotropic power variogram.